Photoluminescent Metal–Sulfur Clusters Derived from Tetrathiometalates: Metal-to-Metal Charge-Transfer Excited States of d^0–d^{10} Heterobimetallic Sulfido Clusters with Bulky Phosphine Ligands

Chi-Ming Che,*[a] Bao-Hui Xia,[a] Jie-Sheng Huang,*[a] Chi-Keung Chan,[a] Zhong-Yuan Zhou,[b] and Kung-Kai Cheung[a]

Abstract: Reactions of MS_4^{2-} (M = Mo, W) with M′(PCy$_3$)X (M′ = Ag/Au, X = ClO_4/Cl) and $[Cu_2(dcpm)_2(MeCN)_2](ClO_4)_2$ (dcpm = bis(dicyclohexylphosphino)methane) afforded heterometallic sulfido clusters $[M'_2(PCy_3)_2(MS_4)]$ (M = Mo, M′ = Au: **2**; M = W, M′ = Ag: **3**, Au: **4**) and $[Cu_4(dcpm)_4(MS_4)](ClO_4)_2$ (M = Mo: **5**·$(ClO_4)_2$, W: **6**·$(ClO_4)_2$), all of which, except **4**, have been characterized by X-ray structure determination. Clusters **5**·$(ClO_4)_2$ and **6**·$(ClO_4)_2$ feature unusual 16-membered $\{Cu_4P_8C_4\}$ metallamacrocycles formed on the respective tetrathiometalate anion templates and have unusually long Cu–S bonds and Cu···M distances for metal–sulfur clusters that contain a saddle-shaped $\{Cu_4MS_4\}$ core. Low-energy absorption bands are observed in their electronic spectra at ~562 and 467 nm, respectively, assignable to MMCT transitions; quasireversible reduction waves are observed with $E_{1/2} = -1.43$ (**5**$^{2+}$) and −1.78 V (**6**$^{2+}$) versus $FeCp_2^{0/+}$; and they are emissive either in the solid state or in solution. The emission of **6**$^{2+}$ can be quenched by both electron acceptors, such as methylviologen, or electron donors, such as aromatic amines, with the excited state reduction potential E(**6**$^{2+*}$/**6**$^{+}$) estimated to be ~1.13 V versus a normal hydrogen electrode.

Keywords: cluster compounds · luminescence · photochemistry · structure elucidation · tetrathiometalates

Introduction

The utilization of tetrathiometalates (MS_4^{n-}) as precursors for cluster synthesis has resulted in the formation of a vast number of heterometallic sulfido clusters with extraordinary structural varieties.[1] While these clusters have been extensively investigated for the development of structural/functional models for the active sites of enzymes such as nitrogenase,[1b,c,e,g, 2, 3] for seeking new classes of nonlinear optical materials,[1f] and for unearthing the versatile binding behavior of MS_4^{n-} as multidentate ligands,[1a,d] their photophysical and photoredox properties remain essentially unexplored. This is in contrast to the case of *homometallic* sulfido clusters, whose photophysical properties are receiving increasing attention.[4, 5]

In an effort to uncover a photoluminescent *heterometallic* sulfide cluster derived from MS_4^{n-}, we found that a W-Cu-S "fly-wheel" cluster, $[Cu_3(dppm)_3(WS_4)]ClO_4$ (**1**·ClO_4, dppm = bis(diphenylphosphino)methane), is photoluminescent in the solid state.[6] However, when cluster **1**·ClO_4 is dissolved in solution, it exhibits no observable photoluminescence. Hence, our quest for a MS_4^{n-}-derived heterometallic cluster that is emissive in both the solid state and solution media continues. In this context, we draw attention to the d^0–d^{10} heterobimetallic clusters of the general formulation $[M'_xL_y(MS_4)]^{x-2}$ formed from $M^{VI}S_4^{2-}$ (M = Mo, W) and the coinage metal ions M'^{I} (M′ = Cu, Ag, Au) with L being a bulky electron-rich phosphine, such as tricyclohexylphosphine (PCy_3) and bis(dicyclohexylphosphino)methane (dcpm). The present work describes the synthesis, crystal structure, spectroscopy, and photophysical/photoredox properties of several examples of $[M'_xL_y(MS_4)]^{x-2}$ clusters, namely, $[M'_2(PCy_3)_2(MS_4)]$ (M = Mo, M′ = Au: **2**; M = W, M′ = Ag: **3**, Au: **4**) and $[Cu_4(dcpm)_4(MS_4)](ClO_4)_2$ (M = Mo: **5**·$(ClO_4)_2$, W: **6**·$(ClO_4)_2$). Remarkably, clusters **5**·$(ClO_4)_2$ and **6**·$(ClO_4)_2$ are photoluminescent both in the solid state and in solution, which, to our knowledge, constitute the first MS_4^{n-}-derived metal–sulfur clusters that have this property. Further, the electronic spectra of **5**·$(ClO_4)_2$ and **6**·$(ClO_4)_2$ show low-energy bands that probably originate from metal-to-metal

[a] Prof. C.-M. Che, Dr. J.-S. Huang, B.-H. Xia, Dr. C.-K. Chan, Dr. K.-K. Cheung
Department of Chemistry
The University of Hong Kong, Pokfulam Road (Hong Kong)
Fax: (+852) 2857-1586
E-mail: cmche@hku.hk

[b] Prof. Z.-Y. Zhou
Department of Applied Biology and Chemical Technology
The Hong Kong Polytechnic University
Hung Hom, Kowloon (Hong Kong)

0947-6539/01/0718-3998 $ 17.50+.50/0

charge-transfer (MMCT) transitions, a type of CT band that is rarely observed for metal–sulfur clusters[6, 7] although well documented for other types of polynuclear metal complexes.[8]

Results

Syntheses: Treatment of the ammonium salts of tetrathiometalates MS_4^{2-} (M = Mo/W) with two equivalents of $M'(PCy_3)X$ (M′ = Ag/Au, X = ClO_4/Cl) in dichloromethane at room temperature for several hours readily afforded clusters **2**–**4** in 43–78% yields [Reaction (1) in Scheme 1]. Reaction of the same tetrathiometalates with ~2 equivalents of $[Cu_2(dcpm)_2(MeCN)_2](ClO_4)_2$ in acetonitrile at room temperature under nitrogen for 24 h led to isolation of clusters $\mathbf{5}\cdot(ClO_4)_2$ or $\mathbf{6}\cdot(ClO_4)_2$ in ~88% yields [Reaction (2) in Scheme 1]. Clusters **2**–**4**, $\mathbf{5}\cdot(ClO_4)_2$, and $\mathbf{6}\cdot(ClO_4)_2$ contribute the first examples of heterobimetallic sulfido clusters formed from MoS_4^{2-}/WS_4^{2-} and coinage metal ions that bear *bulky* phosphine ligands. Previously, a number of their analogues have been reported, including $[M'_2L_y(MS_4)]$ (y = 2–4),[1a,d, 9] $[Cu_3(PPh_3)_3Cl(MS_4)]$,[1d] $[M'_4L_y(MS_4)_2]$ (y = 4, 8),[1d, 10] $(n\text{Bu}_4\text{N})[Cu_3(dppm)_2Br_2(WS_4)]$,[11] $\mathbf{1}\cdot X$ (X = PF_6, Br),[11] and $[Cu_4(dppm)_4(MS_4)](PF_6)_2$ (M = Mo: $\mathbf{5}'\cdot(PF_6)_2$, W: $\mathbf{6}'\cdot(PF_6)_2$),[11] as well as $\mathbf{1}\cdot ClO_4$;[6] however, all the phosphine ligands in these clusters have considerably smaller cone angles.[12]

The formation of $[Cu_4(dcpm)_4(MS_4)]^{2+}$ (M = Mo: $\mathbf{5}^{2+}$, W: $\mathbf{6}^{2+}$) from Reaction (2) in fairly high yields is particularly interesting. First, we have demonstrated that a similar reaction of WS_4^{2-} with $[Cu_2(dppm)_2(MeCN)_4](ClO_4)_2$ affords the tetranuclear cluster $\mathbf{1}\cdot ClO_4$ in 25% yield [Reaction (3) in Scheme 1];[6] no $[Cu_4(dppm)_4(WS_4)]^{2+}$ ($\mathbf{6}'^{2+}$), the dppm counterpart of the pentanuclear cluster $\mathbf{6}^{2+}$, is obtained from the reaction. Likewise, we could not isolate the dcpm counterpart of $[Cu_3(dppm)_3(WS_4)]^+$ ($\mathbf{1}^+$) from Reaction (2). Second, although $\mathbf{6}'^{2+}$ has recently been prepared from a solid-state reaction at elevated temperature [Reaction (4) in Scheme 1],[11] the yield of the cluster is 22%; when the same reaction is carried out in solution, cluster $\mathbf{1}^+$ rather than $\mathbf{6}'^{2+}$ is obtained [Reaction (5) in Scheme 1].[11] These observations clearly reveal a dramatic influence of the steric/electronic properties of the phosphine ligands on the formation of this type of metal–sulfur cluster.

^{31}P NMR spectra: Clusters **2**–**4**, $\mathbf{5}\cdot(ClO_4)_2$, and $\mathbf{6}\cdot(ClO_4)_2$ each exhibit a ^{31}P NMR spectrum that shows a single phosphorus environment. The signals of all the clusters except **3** appear as singlets with δ of 66.98 (**2**), 66.88 (**4**), 6.44 ($\mathbf{5}\cdot(ClO_4)_2$), and 6.58 ($\mathbf{6}\cdot(ClO_4)_2$). In the case of **3**, the spectrum at room temperature features a well-separated doublet in 1:1 ratio centered at δ = 49.7 with J = 576 Hz as a result of the ^{31}P–$^{107/109}$Ag spin–spin coupling (the ^{31}P–^{107}Ag and ^{31}P–^{109}Ag couplings are not resolved under the NMR conditions). This is different from a PPh_2Me analogue of **3**, in which case the P–Ag couplings are not observed at room temperature due to a rapid exchange of the phosphine ligands.[10a]

X-ray crystal structures: All the new clusters, except **4**, have been structurally characterized by X-ray crystallography. The crystal data and structure refinement are summarized in Table 1. Because **2** and **3** or $\mathbf{5}\cdot(ClO_4)_2$ and $\mathbf{6}\cdot(ClO_4)_2$ belong to the same structure type, only the ORTEP drawings of **3** and $\mathbf{6}\cdot(ClO_4)_2$ are shown here (see Figure 1 and Figure 2, respectively). As expected, the tetrathiometalate units in these clusters are very similar; each of them essentially adopts a tetrahedral geometry.

Cluster **3** represents the only example of structurally characterized linear $[Ag_2L_2(MS_4)]$ clusters, with L being phosphine ligands, in which both the Ag atoms are three-coordinate. Previously, Müller and coworkers reported the structure of $[Ag_2(PPh_3)_3(MoS_4)]\cdot 0.8\,CH_2Cl_2$ ($\mathbf{7}\cdot 0.8\,CH_2Cl_2$), which contains both three- and four-coordinate Ag atoms.[13] Although **3** bears a bulky phosphine ligand, the metrical parameters of both the $\{(Cy_3P)Ag(\mu\text{-}S)_2W\}$ halves are similar to those of the

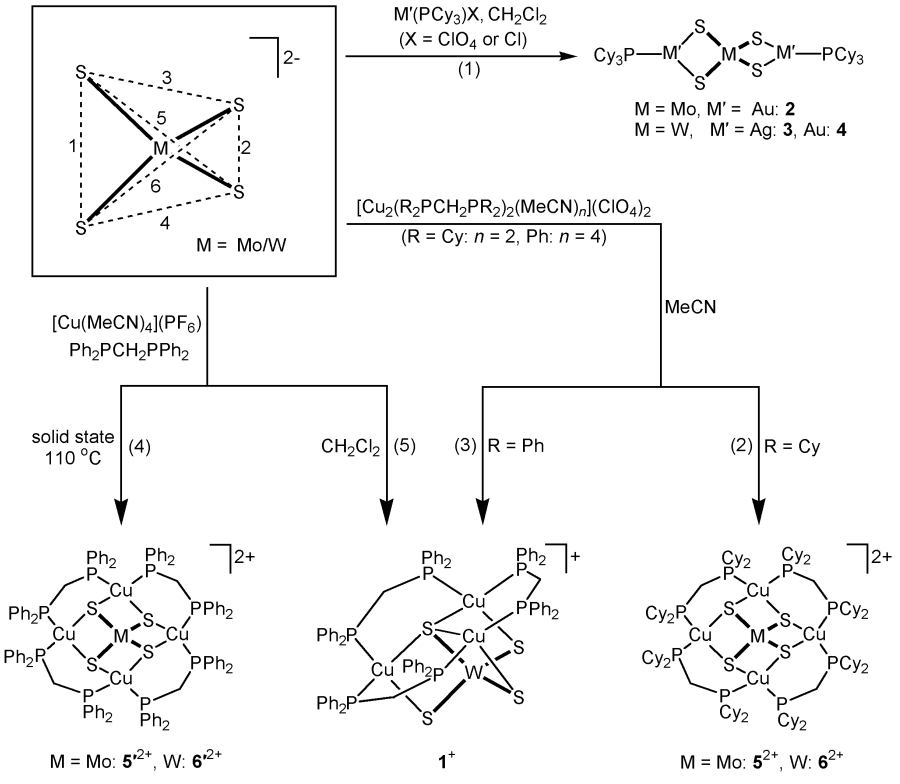

Scheme 1. Syntheses of **2**–**4**, $\mathbf{5}\cdot(ClO_4)_2$, and $\mathbf{6}\cdot(ClO_4)_2$. The syntheses of $\mathbf{1}\cdot ClO_4$ (ref. [6]), $\mathbf{1}\cdot PF_6$, $\mathbf{5}'\cdot(PF_6)_2$, and $\mathbf{6}'\cdot(PF_6)_2$ (ref. [11]) are also included for comparison.

Table 1. Crystal data and structure refinement for **2**, **3**, **5**·$(ClO_4)_2$, and **6**·$(ClO_4)_2$.

	2·CH_2Cl_2	**3**·CH_2Cl_2	**5**·$(ClO_4)_2$·2MeCN·2Et_2O	**6**·$(ClO_4)_2$·EtOH
formula	$C_{37}H_{68}Cl_2P_2S_4MoAu_2$	$C_{37}H_{68}Cl_2P_2S_4WAg_2$	$C_{112}H_{210}N_2Cl_2O_{10}P_8S_4MoCu_4$	$C_{102}H_{190}Cl_2O_9P_8S_4WCu_4$
M_R	1263.91	1173.62	2541.82	2445.45
crystal system	triclinic	triclinic	orthorhombic	triclinic
space group	$P\bar{1}$	$P\bar{1}$	*Aba*2	$P\bar{1}$
a [Å]	10.985(2)	10.968(2)	28.91(1)	14.932(6)
b [Å]	12.957(2)	13.056(2)	20.656(7)	14.980(6)
c [Å]	17.893(3)	17.919(3)	21.714(7)	26.49(1)
α [°]	98.98(2)	99.76(2)	90	90.212(8)
β [°]	107.92(2)	106.65(2)	90	90.240(8)
γ [°]	97.08(2)	98.31(2)	90	92.031(9)
V [Å^3]	2353.4(9)	2371.6(9)	12967(7)	5922(4)
Z	2	2	4	2
ρ_{calcd} [Mg m^{-3}]	1.783	1.643	1.302	1.372
$\mu(Mo_{K\alpha})$ [cm^{-1}]	68.85	36.17	9.95	19.48
F(000)	1236	1172	5408	2564
reflections collected	26100	24045	43027	38872
independent reflections	7988	8095	14759	26745
parameters	418	428	631	1117
goodness of fit	1.63	1.55	0.749	0.801
final *R* indices [$I > 2\sigma(I)$]	$R1^{[a]} = 0.040$	$R1^{[a]} = 0.042$	$R1 = 0.043$	$R1 = 0.062$
	$wR^{[a]} = 0.059$	$wR^{[a]} = 0.057$	$wR2 = 0.11$	$wR2 = 0.16$
largest difference peak/hole [e Å^{-3}]	1.45/ − 3.38	0.64/ − 2.20	0.69/ − 0.50	0.98/ − 0.93

[a] [$I > 3\sigma(I)$].

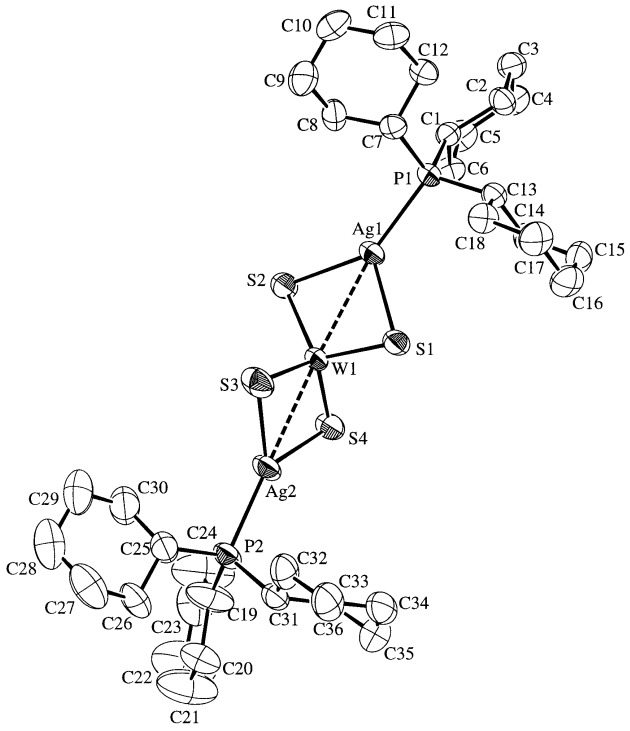

Figure 1. ORTEP drawing of **3** with thermal ellipsoids on the 40% probability level (hydrogen atoms are not shown). Average Ag···W distance: 2.8951(5) Å. Selected average bond lengths [Å]: W–S 2.206(2), Ag–S 2.475(2), Ag–P 2.373(2). Selected average bond angles [°]: S-W-S 109.48(8), S-Ag-S 95.43(6), Ag-S-W 76.16(6), S-Ag-P 132.19(7).

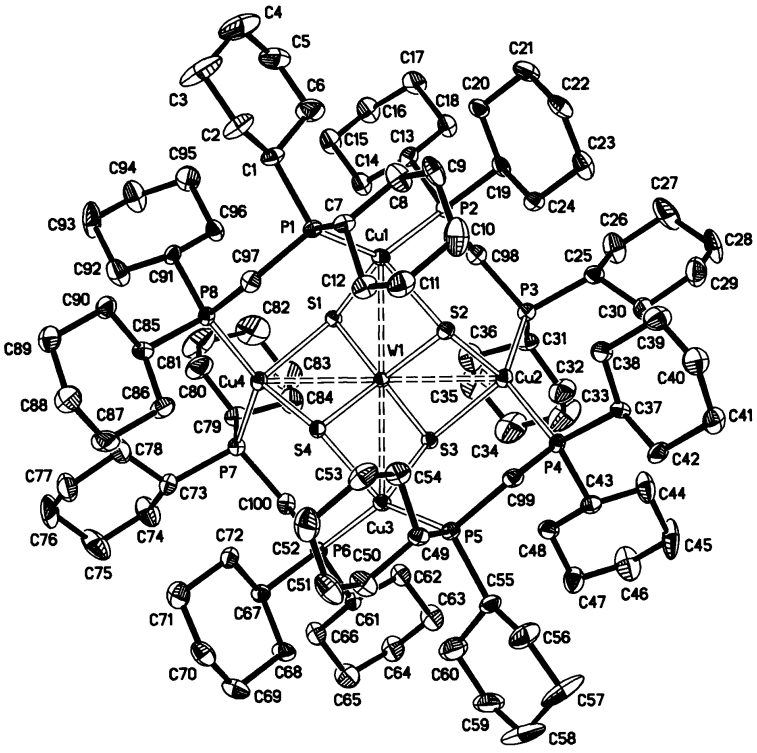

Figure 2. ORTEP drawing of **6**·$(ClO_4)_2$ with thermal ellipsoids on the 50% probability level (the ClO_4^- counteranions and hydrogen atoms are not shown). Average Cu···W distance: 2.857(1) Å. Selected average bond lengths [Å]: W–S 2.204(1), Cu–S 2.406(1), Cu–P 2.301(1). Selected average bond angles [°]: S-W-S 109.48(4), S-Cu-S 96.08(4), Cu-S-W 76.45(4), Cu-S-Cu 115.66(4), S-Cu-P 104.88(5), P-Cu-P 134.63(4).

$\{(Ph_3P)Ag(\mu\text{-}S)_2Mo\}$ moiety of **7** with a three-coordinate Ag atom. Likewise, the structure of **2** is similar to those of its PPh_3[9c] and PEt_3[9b] counterparts reported in the literature.

In contrast, the saddle-shaped $\{Cu_4MS_4\}$ cores in $\mathbf{5}^{2+}$ and $\mathbf{6}^{2+}$ have appreciably different geometries from those in $\mathbf{5}'^{2+}$ and $\mathbf{6}'^{2+}$,[11] and in all the other $[Cu_4MS_4]$-containing polymeric or discrete clusters including $\{(Ph_4P)_2[Cu_4Br_4(MoS_4)]\}_n$,[14a] $(Bu_4N)_2[Cu_4Cl_4(MoS_4)]$,[14e] $\{(Et_4N)_2[Cu_4X_4(MoS_4)]\}_n$ (X = NCS,[14d] CN[14g]), $(Et_4N)_4[Cu_4I_6(MoS_4)]$,[14f] $\{Y_2[Cu_4(NCS)_4(WS_4)]\}_n$ (Y = Me_4N,[14b] Et_4N,[14d] Ph_4P[14c]), $\{(Et_4N)_2[Cu_4$-

0947-6539/01/0718-4000 $ 17.50+.50/0 *Chem. Eur. J.* **2001**, *7*, No. 18

$(CN)_4(WS_4)]\}_n$,[14g] and $\{(Et_4N)_3[Cu_4(NCS)_5(WS_4)]\}_n$.[14d] For example, the average Cu–S bond lengths of 2.378 ($\mathbf{5}^{2+}$) and 2.406 Å ($\mathbf{6}^{2+}$) and the average Cu ··· M (M = Mo, W) distances of 2.827 ($\mathbf{5}^{2+}$) and 2.857 Å ($\mathbf{6}^{2+}$) are all longer than the respective bond lengths or distances in any of the other $\{Cu_4MS_4\}$-containing clusters mentioned above, which range from 2.242 to 2.351 Å (Cu-S) and from 2.609 to 2.778 Å (Cu ··· M).[11, 14] Notably, replacing the phenyl groups in $\mathbf{5}'^{2+}$/$\mathbf{6}'^{2+}$ with the cyclohexyl groups to form $\mathbf{5}^{2+}$/$\mathbf{6}^{2+}$ results in an increase of the average closest Cu ··· Cu distances from 3.88 to 4.03 Å ($\mathbf{5}'^{2+} \rightarrow \mathbf{5}^{2+}$) and from 3.90 to 4.07 Å ($\mathbf{6}'^{2+} \rightarrow \mathbf{6}^{2+}$).

Electronic spectra: Figure 3 depicts the UV/Visible absorption spectra of clusters **2**–**4**, $\mathbf{5}\cdot(ClO_4)_2$, and $\mathbf{6}\cdot(ClO_4)_2$, together with those of the respective tetrathiometalates MoS_4^{2-} and WS_4^{2-}. The spectral data of these compounds are listed in Table 2. As shown in Figure 3, either MoS_4^{2-} or WS_4^{2-} exhibits a spectrum featuring three intense bands $\nu_1 - \nu_3$ in the 210 – 700 nm region. The formation of the trinuclear clusters **2**–**4** from MoS_4^{2-} or WS_4^{2-} causes some changes in the intensity and location of these bands, but retains the main features of the spectra. However, coordination of MoS_4^{2-} or WS_4^{2-} to copper(I) ions to form the pentanuclear cluster $\mathbf{5}^{2+}$ or $\mathbf{6}^{2+}$ renders the spectrum more complicated, with the appearance of new bands at about 357 and 562 nm for $\mathbf{5}^{2+}$, and 324 and 467 nm for $\mathbf{6}^{2+}$. These new bands show little solvent dependence among the three solvents examined (see Table 2).

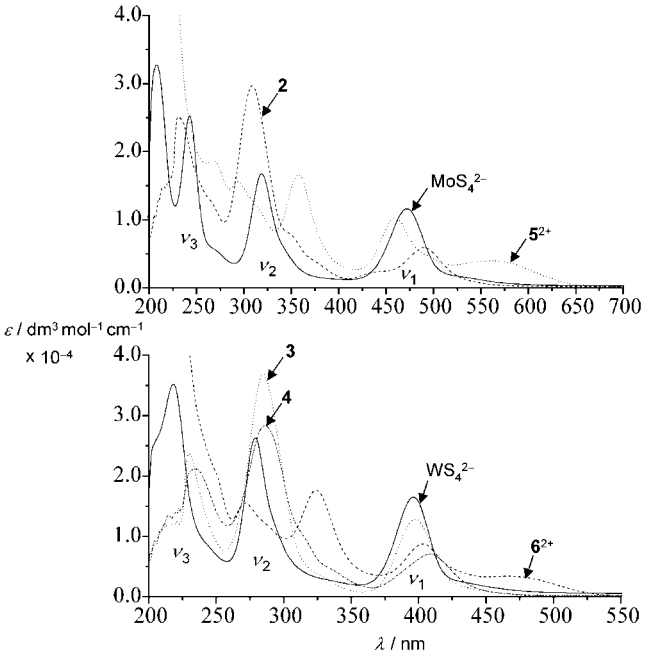

Figure 3. UV-visible spectra of **2**–**4** (in CH_2Cl_2), $\mathbf{5}\cdot(ClO_4)_2$ and $\mathbf{6}\cdot(ClO_4)_2$ (in MeCN); those of MoS_4^{2-} and WS_4^{2-} (in MeOH) are shown for comparison. Note that the spectra of $\mathbf{5}\cdot(ClO_4)_2$ and $\mathbf{6}\cdot(ClO_4)_2$ in MeCN are similar to those in CH_2Cl_2 or MeOH (see Table 2).

Table 2. UV/Vis spectral data for **2**–**4**, $\mathbf{5}\cdot(ClO_4)_2$, and $\mathbf{6}\cdot(ClO_4)_2$ at 298 K. The data for the ammonium salts of tetrathiometalates MoS_4^{2-} and WS_4^{2-} are also included for comparison.

cluster	solvent	λ_{max} [nm] ($\varepsilon \times 10^{-3}$ [dm^3 mol^{-1} cm^{-1}])[a]
		MoS_4^{2-} and its derivatives
MoS_4^{2-}	MeOH	243(25.2), 319(16.8), 472(11.6)
2	CH_2Cl_2	231(25.1), *266(12.6)*, 309(29.7), *351(6.8)*, *377(3.2)*, *436(1.9)*, 490(5.3)
$\mathbf{5}^{2+}$	MeCN	267(18.7), 294(15.6), *314(11.9)*, 357(16.6), 460(9.8), *495(4.4)*, 562(3.8)
	MeOH	267(18.7), 295(15.4), *314(11.9)*, 357(16.4), 460(9.5), *495(4.3)*, 561(3.6)
	CH_2Cl_2	268(19.7), 295(16.4), *314(12.6)*, 358(17.5), 459(10.0), *495(4.5)*, 562(3.8)
		WS_4^{2-} and its derivatives
WS_4^{2-}	MeOH	218(35.2), 279(26.3), 396(16.5)
3	CH_2Cl_2	230(23.8), 285(36.8), *330(2.6)*, 397(9.7)
4	CH_2Cl_2	234(21.2), 286(28.3), *317(8.4)*, *339(3.7)*, 408(6.5)
$\mathbf{6}^{2+}$	MeCN	272(15.5), 324(17.7), 403(8.8), 467(3.3)
	MeOH	272(15.0), 325(17.4), 404(8.7), 468(3.4)
	CH_2Cl_2	272(16.5), 325(18.7), 405(8.8), 468(3.3)

[a] The data for shoulders are set italic.

Photophysical properties: Cluster $\mathbf{6}\cdot(ClO_4)_2$ exhibits an intense orange emission at 298 K with $\lambda_{max} = \sim 619$ nm in the solid state and in solution. The emission of cluster $\mathbf{5}\cdot(ClO_4)_2$ at the same temperature is relatively weak, with λ_{max} located at longer wavelengths ($\sim$727 nm in the solid state and 709 nm in solution). None of clusters **2**–**4** was found to be photoluminescent.

Table 3 shows the photophysical properties of $\mathbf{5}\cdot(ClO_4)_2$ and $\mathbf{6}\cdot(ClO_4)_2$ in various media and at different temperatures. The emission spectra of $\mathbf{6}\cdot(ClO_4)_2$ in a glassy state (MeOH/EtOH 4:1, v/v) at 77 K and in acetonitrile at 298 K, together with its excitation/absorption spectrum under these conditions, are depicted in Figure 4. As shown in Table 3, the emission life times (τ) of $\mathbf{5}^{2+}$ and $\mathbf{6}^{2+}$ in solution are fairly long, ranging from 0.8 – 1.5 μs for the three solvents examined. Further, for both $\mathbf{5}^{2+}$ and $\mathbf{6}^{2+}$, lowering the temperature from 298 to 77 K significantly red shifts their emission bands.

Table 3. Photophysical properties of $\mathbf{5}\cdot(ClO_4)_2$ and $\mathbf{6}\cdot(ClO_4)_2$.

medium	T [K]	λ_{max} [nm]		τ [μs]		quantum yield	
		$\mathbf{5}^{2+}$	$\mathbf{6}^{2+}$	$\mathbf{5}^{2+}$	$\mathbf{6}^{2+}$	$\mathbf{5}^{2+}$	$\mathbf{6}^{2+}$
MeCN	298	709	619	1.1	1.5	4.3×10^{-4}	0.017
MeOH	298	709	619	1.1	1.2	4.7×10^{-4}	0.014
CH_2Cl_2	298	709	619	0.8	0.8	2.9×10^{-4}	0.010
solid	298	727	619		7.8		
solid	77	800	665		58.0		
MeOH/EtOH (4:1, v/v)	77	800	667		56.0		

Electrochemistry of clusters $\mathbf{5}\cdot(ClO_4)_2$ and $\mathbf{6}\cdot(ClO_4)_2$: The cyclic voltammograms of $\mathbf{5}^{2+}$ and $\mathbf{6}^{2+}$ in acetonitrile show *quasi-reversible* reduction waves at $E_{1/2} = -1.43$ and -1.78 V versus $FeCp_2^{0/+}$, respectively.[15] These potentials are less negative than the reduction potentials (versus $FeCp_2^{0/+}$) reported for the respective tetrathiometalates (MoS_4^{2-}: -2.60 V in MeCN,[16] WS_4^{2-}: -3.16 V in DMF[17]). The more negative

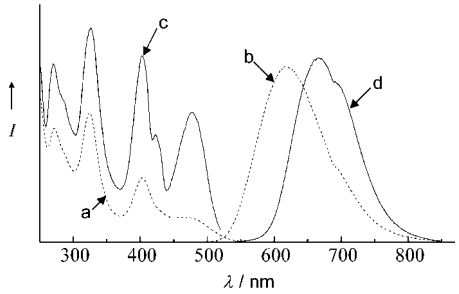

Figure 4. a) Absorption and b) emission spectra in MeCN at 298 K, and c) excitation and d) emission spectra of $\mathbf{6}\cdot(ClO_4)_2$ in a glassy state (MeOH/EtOH 4:1, v/v) at 77 K. I = intensity.

reduction potential obtained for the tungsten cluster ($\mathbf{6}^{2+}$) than for the molybdenum cluster ($\mathbf{5}^{2+}$) is parallel to the results found for related clusters such as $[Co(MS_4)_2]^{2-}$ (M = Mo, W).[1d] Note that of the other structurally characterized $\{Cu_4MS_4\}$-containing clusters[11, 14] described above, only $(Et_4N)_4[Cu_4I_6(MoS_4)]$[14f] has been studied by cyclic voltammetry; however, this compound exhibits *irreversible* reduction waves in solution.

Quenching of the emission of cluster $\mathbf{6}\cdot(ClO_4)_2$: The emission of $\mathbf{6}^{2+}$ can be quenched by both electron acceptors such as MV^{2+} (methylviologen, i.e., 1,1′-dimethyl-4,4′-bipyridinium dichloride) and electron donors such as TMPD (*N*,*N*,*N*′,*N*′-tetramethyl-*p*-phenylenediamine), with MV^{2+} and TMPD converted to $MV^{\bullet+}$ and $TMPD^{\bullet+}$, respectively.[18] Transient absorption spectroscopic studies reveal that the quenching obeys the Stern–Volmer equation in the range of the quencher concentrations employed, and the quenching rate constants after diffusional effect correction (kq') are determined to be 1.2×10^7 dm^{3}mol^{-1}s^{-1} for MV^{2+} and 2.00×10^6–2.92×10^9 dm^{3}mol^{-1}s^{-1} for a series of aromatic amine donors (including TMPD) with similar sizes and electronic structures but different redox potentials $E(D^+/D^0)$ (see Table 4).

Discussion

Tetrathiometalates as anion templates for metallamacrocycle formation: Since the pioneering work by Müller and coworkers in early 1970s,[19] tetrathiometalates have been widely known as versatile multidentate ligands in metal complex formation.[1] Indeed, as shown in Scheme 1, clusters $\mathbf{1}^+$,[6] **2**–**4**, $\mathbf{5}^{2+}$, and $\mathbf{6}^{2+}$ can be well described as coinage metal complexes with MoS_4^{2-} or WS_4^{2-} as ligands formed by coordination of the coinage metal ions to the pairs of sulfido groups on edges 1 and 2 (**2**–**4**), 1, 3, and 5 ($\mathbf{1}^+$), and 1–4 ($\mathbf{5}^{2+}$, $\mathbf{6}^{2+}$) of the MS_4^{2-} tetrahedron.

We notice that the structures of $\mathbf{1}^+$, $\mathbf{5}^{2+}$, and $\mathbf{6}^{2+}$ contain macrocycle moieties: a tridentate 12-membered $\{Cu_3P_6C_3\}$ ring in $\mathbf{1}^+$ and a tetradentate 16-membered $\{Cu_4P_8C_4\}$ ring in $\mathbf{5}^{2+}$ or $\mathbf{6}^{2+}$. The conformation of the $\{Cu_4P_8C_4\}$ macrocycle in $\mathbf{6}^{2+}$ is shown in Figure 5. Because these macrocycles are bound to MoS_4^{2-} or WS_4^{2-} and are formed from simpler copper compounds in the presence of the tetrathiometalates [Reactions (2) and (3) in Scheme 1], we highlight here the function of tetrathiometalates MS_4^{n-} as a new class of *anion template* for macrocycle formation.[20] The $\{Cu_3P_6C_3\}$ or $\{Cu_4P_8C_4\}$ macrocycles might have intrinsic stability in view of their previous appearance in other types of polynuclear copper complexes including $[Cu_3(dppm)_3X_2]^+$ (X = Cl,[21a] PhC_2[21d]), $[Cu_3(dppm)_3X]^{2+}$ (X = OH,[21b] PhC_2[21c]), $[Cu_4(dppm)_4(CS_3)_2]$ (**8a**),[22a] and $[Cu_4(dppm)_4E]^{2+}$ (E = S: **8b**,[22b] C_2: **8c**[22c]), and in clusters $\mathbf{5}'^{2+}$ and $\mathbf{6}'^{2+}$.[11] Notably, the $\{Cu_4P_8C_4\}$ macrocycles generated on templates MoS_4^{2-} and WS_4^{2-}, as in clusters $\mathbf{5}^{2+}$ and $\mathbf{6}^{2+}$, have substantially larger Cu_4 cavities than those in **8a**–**c**. For example, the average closest Cu···Cu distances in $\mathbf{5}^{2+}$ (4.03 Å) and $\mathbf{6}^{2+}$ (4.07 Å) are much longer than those in **8a**–**c** (2.87–3.31 Å)[22] and are the longest ever found for the compounds bearing the $\{Cu_4P_8C_4\}$ macrocycles (Figure 6). Such a wide range of Cu···Cu distances (2.87 to 4.07 Å) observed for the $\{Cu_4P_8C_4\}$ rings demonstrates that this class of metallamacrocycles are remarkably flexible in anion binding, and should be able to form stable complexes with diverse types of anions.

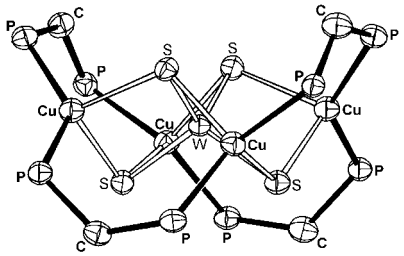

Figure 5. The core structure of $\mathbf{6}^{2+}$ showing the conformation of the 16-membered $\{Cu_4P_8C_4\}$ ring.

The markedly longer Cu–S bonds and Cu···M (M = Mo or W) distances in clusters $\mathbf{5}^{2+}$ and $\mathbf{6}^{2+}$ than in $\mathbf{5}'^{2+}$ and $\mathbf{6}'^{2+}$ (see above) indicate that the binding of the $\{Cu_4P_8C_4\}$ macrocycle with MoS_4^{2-}/WS_4^{2-} in $\mathbf{5}^{2+}/\mathbf{6}^{2+}$ is weaker than in $\mathbf{5}'^{2+}/\mathbf{6}'^{2+}$, probably arising from the sterically more demanding and/or more electron-rich nature of the dcpm than the dppm ligand. In fact, $\mathbf{5}^{2+}$ and $\mathbf{6}^{2+}$ have the weakest interaction between tetrathiometalate and copper ions among all the clusters bearing the $\{Cu_4MS_4\}$ cores, as reflected from their Cu–S bond lengths and Cu···M distances. Perhaps owing to this property, the electronic spectra of $\mathbf{5}^{2+}$ and $\mathbf{6}^{2+}$ (Figure 3) are somewhat reminiscent of those of MoS_4^{2-} or WS_4^{2-}.

Table 4. Rate constants for the quenching of the emission of $\mathbf{6}\cdot(ClO_4)_2$ by aromatic amine donors in acetonitrile at 298 K.

aromatic amine	$E(D^+/D^0)$[a]	k_q[b]	k_q'[c]	$\ln k_q'$
TMPD	0.35	2.55×10^9	2.92×10^9	21.79
p-phenylenediamine	0.53	8.35×10^8	8.71×10^8	20.59
N,*N*,*N*′,*N*′-tetramethylbenzidine	0.67	1.38×10^9	1.48×10^9	21.12
o-phenylenediamine	0.75	1.55×10^8	1.56×10^8	18.86
benzidine	0.79	4.81×10^7	4.82×10^7	17.69
phenothiazine	0.86	1.86×10^7	1.86×10^7	16.74
diethylaniline	0.94	5.00×10^6	5.00×10^6	15.42
diphenylamine	1.07	2.00×10^6	2.00×10^6	14.51

[a] V versus NHE (from ref. [29]). [b] The rate constant [dm^{3}mol^{-1}s^{-1}] obtained according to Stern–Volmer equation. [c] The rate constant [dm^3 mol^{-1}s^{-1}] corrected for diffusional effects ($1/k_q' = 1/k_q - 1/k_d$, in which k_d is taken to be 2.0×10^{10} dm^{3}mol^{-1}s^{-1}).

0947-6539/01/0718-4002 $ 17.50+.50/0 *Chem. Eur. J.* **2001**, *7*, No. 18

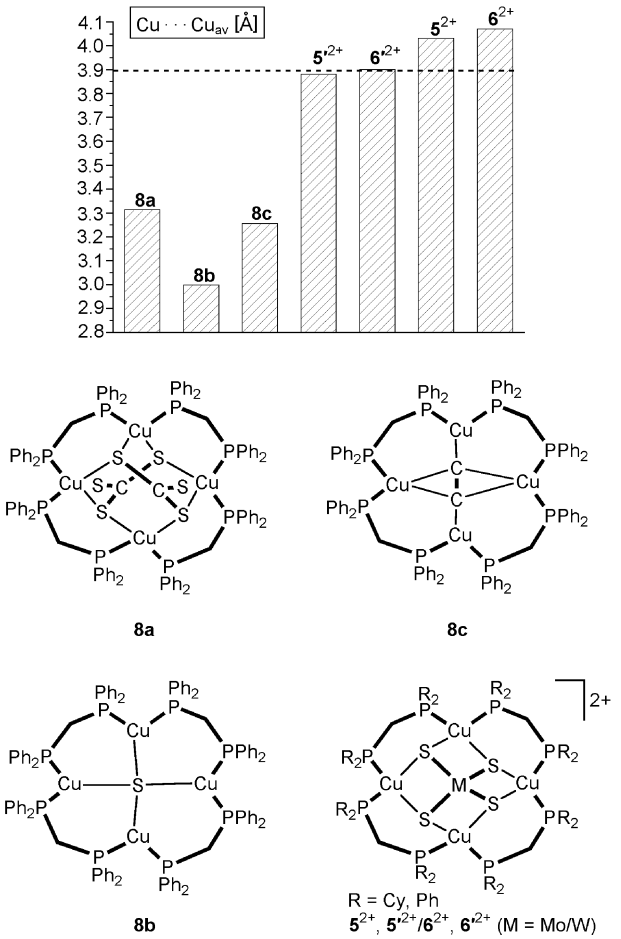

Figure 6. Comparison of the average Cu ··· Cu distances between adjacent copper atoms in the 16-membered $\{Cu_4P_8C_4\}$ ring coordinated to various anions.

Metal-to-metal charge-transfer (MMCT) excited states: MMCT transitions of heteronuclear metal complexes that contain both reducing and oxidizing metal centers bridged by *non-sulfido* ligands (such as cyanide) have been extensively studied by Vogler and co-workers.[8] In contrast, very few metal – sulfur clusters have been found to exhibit MMCT transitions. Several years ago, Kaim and co-workers proposed that the low-energy bands at $\lambda_{max} = 500$ and 600 nm in the electronic spectra of the homometallic clusters $[Re(CO)_3Cl(ReS_4)]$ and $[Re_2(CO)_6Cl_2(ReS_4)]$, respectively, originate from $Re^{I} \rightarrow Re^{VII}$ MMCT transitions.[7] Recently, we observed that the structurally characterized heterometallic cluster **1**·ClO_4 exhibits a low-energy absorption band ($\lambda_{max} = 465$ nm, $\varepsilon = 3600$) that can be assigned to the $[\psi(Cu,P) \rightarrow \sigma^*(W\text{-}S)]$ MMCT transitions on the basis of extended Hückel molecular-orbital calculations.[6] Since **2** – **4**, **5**$^{2+}$, and **6**$^{2+}$, like **1**$^{+}$, are all $d^0 - d^{10}$ heterobimetallic sulfido clusters bearing phosphine ligands, we wanted to find out whether they exhibit observable MMCT transitions as well.

Clusters **2** – **4** feature the electronic spectra similar to those of respective tetrathiometalates MoS_4^{2-} and WS_4^{2-}, suggesting that the intense absorption bands observed for these clusters basically originate from the internal electron transitions of their tetrathiometalate moieties (the ν_1 and ν_2 bands of MoS_4^{2-}/WS_4^{2-} as shown in Figure 3 are assigned to LMCT transitions by Müller et al.,[1a] and Kaim et al.[23]). This is supported by the lack of significant lower energy absorptions for the silver(I) phosphine complexes $[Ag(PR_3)_2]ClO_4$ and $Ag(PR_3)(O_2CCF_3)$ (R = Me or Cy) ($\varepsilon < 10^2$ at $\lambda > 250$ nm),[24] and by the appearance of appreciable absorptions only at $\lambda <$ 260 nm for the gold(I) phosphine complex $[Au(PEt_3)_2]^+$ ($\varepsilon < 2 \times 10^3$ at $\lambda = 220 - 260$ nm).[25] The shift of the absorption bands of MoS_4^{2-} or WS_4^{2-} upon formation of **2** – **4** probably arises from the interaction between the tetrathiometalate and the $M'(PCy_3)$ (M′ = Ag, Au) groups (such interactions should perturb the molecular orbitals of the tetrathiometalates). We note that clusters **2** – **4** exhibit some poorly resolved shoulders that are absent in the spectra of MoS_4^{2-} and WS_4^{2-}. The shoulders at 351, 377 nm for **2**, 330 nm for **3**, and 317, 339 nm for **4** are located at energies that seem too high for MMCT transitions of these clusters and we tentatively assign these bands to the p(P) → d(M) (M = Mo or W) transitions.

With regard to clusters **5**$^{2+}$ and **6**$^{2+}$, the bands at 460, 294 nm for **5**$^{2+}$ and 403, 272 nm for **6**$^{2+}$ are comparable to the ν_1, ν_2 bands of MoS_4^{2-} or WS_4^{2-} and the corresponding bands of **2** – **4** (see Figure 3), and could be assigned to the internal electron transitions of their tetrathiometalate moieties, whose molecular orbitals are somewhat perturbed by the interaction with the $\{Cu_4P_8C_4\}$ macrocycles. The intense higher energy new bands at 357 (**5**$^{2+}$) and 324 nm (**6**$^{2+}$) are located at wavelengths comparable to those of the poorly resolved shoulders of **2** – **4** described above; we again tentatively assign these bands to the p(P) → d(M) (M = Mo or W) transitions.

The appearance of broad, low-energy new bands at ~562 nm ($\varepsilon = 3800$, in MeCN) for **5**$^{2+}$ and ~467 nm ($\varepsilon =$ 3300, in MeCN) for **6**$^{2+}$ is intriguing. We assign these bands to the $[\psi(Cu,P) \rightarrow \sigma^*(M\text{-}S)]$ (M = Mo, W) MMCT transitions for the following reasons. First, like cluster **1**$^{+}$, clusters **5**$^{2+}$ and **6**$^{2+}$ contain both reducing (Cu^{I}) and oxidizing (Mo^{VI} or W^{VI}) metal centers bridged by sulfido ligands; this may allow MMCT transitions to occur upon light absorption.[8] Second, the low-energy bands of the two W-Cu-S clusters **1**$^{+}$ and **6**$^{2+}$ are very similar and, therefore, should have the same origin. Third, the $\{Cu_4P_8C_4\}$ macrocycles in **5**$^{2+}$ and **6**$^{2+}$ are unlikely to show absorption bands in the low-energy region, since the complex $[Cu_2(dcpm)_2(MeCN)_2](ClO_4)_2$ in the same solvent shows absorptions only at $\lambda < 375$ nm.[26] Fourth, complex **8b**, which can be considered as a complex of the $\{Cu_4P_8C_4\}$ macrocycle with sulfido anion (see Figure 6), exhibits no appreciable absorptions at $\lambda > 400$ nm.[22b] Finally, the appearance of the MMCT band at longer wavelength for **5**$^{2+}$ than for **6**$^{2+}$ is consistent with the lower energy of the 4d (Mo) orbital than the 5d (W) orbital. A notable feature of the MMCT bands of **5**$^{2+}$ and **6**$^{2+}$ lies in their virtual independence on the nature of the solvents; this is in contrast to the large solvent effect observed for the MMCT bands of other heteronuclear metal complexes.[27]

Taking into account the lack of photoluminescence and MMCT bands for **2** – **4** and the observation of both photoluminescence and MMCT bands for **1**$^{+}$, **5**$^{2+}$, and **6**$^{2+}$, together with the fairly long emission lifetimes found for **5**$^{2+}$ and **6**$^{2+}$ (Table 3), we propose that the emission of **5**$^{2+}$ and **6**$^{2+}$, like that of **1**$^{+}$ in the solid state,[6] should be phosphorescent in

nature originating from the $^3[\psi(Cu,P)^1\sigma^*(M\text{-}S)^1]$ (M = Mo, W) triplet MMCT excited states, rather than from the ($S^{2-} \rightarrow M^{VI}$) (M = Mo or W) LMCT excited states of their MoS_4^{2-} or WS_4^{2-} moieties. As a matter of fact, neither of the tetrathiometalates is found to be emissive under similar conditions. To our knowledge, clusters $\mathbf{1}^+$, $\mathbf{5}^{2+}$, and $\mathbf{6}^{2+}$ are rare examples of metal–sulfur clusters with emissive MMCT excited states.

Given the similarity between the MMCT bands of $\mathbf{1}^+$ and $\mathbf{6}^{2+}$, and between the emissions of these two W-Cu-S clusters in the solid state, the dramatic difference in their photophysical properties in solution is striking. This could again be rationalized by the sterically more-demanding nature of the dcpm than the dppm ligand. Probably, the emitting $\{Cu_4WS_4\}$ core of $\mathbf{6}^{2+}$ is well protected by the sixteen bulky cyclohexyl groups, which prevents or mitigates the radiationless decay of the excited state through collision with solvent molecules. The limited solvent accessibility of the $\{Cu_4WS_4\}$ core in $\mathbf{6}^{2+}$, and the $\{Cu_4MoS_4\}$ core in $\mathbf{5}^{2+}$ as well, might in part account for the aforementioned small solvent dependence of the MMCT bands observed for these clusters.

Photo-induced electron transfer reactions: The emission of $\mathbf{5}^{2+}$ and $\mathbf{6}^{2+}$ in solution with long emission lifetimes makes these clusters unique candidates for examining the reactivity of the MMCT excited states of d^0-d^{10} heteronuclear metal complexes, an issue that we were unable to address in our previous work on cluster $\mathbf{1}^+$[6] because of its nonemissive nature in solution. As described above, the emission of $\mathbf{6}^{2+}$ can be quenched by the electron acceptor MV^{2+} and a variety of electron donors such as TMPD, indicating that this cluster can act as either a reductant or an oxidant in the excited state. In view of the formation of $MV^{\bullet+}$ and $TMPD^{\bullet+}$ after the quenching, the respective photoredox processes can be described by Reactions (6) and (7):

$$[Cu_4(dcpm)_4(WS_4)]^{2+*}\ (\mathbf{6}^{2+*}) + MV^{2+} \rightarrow [Cu_4(dcpm)_4(WS_4)]^{3+}\ (\mathbf{6}^{3+}) + MV^{\bullet+} \quad (6)$$

$$[Cu_4(dcpm)_4(WS_4)]^{2+*} + TMPD \rightarrow [Cu_4(dcpm)_4(WS_4)]^{+}\ (\mathbf{6}^{+}) + TMPD^{\bullet+} \quad (7)$$

To understand the photoredox behavior of $\mathbf{6}^{2+}$, it is important to know the redox potentials of the excited state $\mathbf{6}^{2+*}$, namely, $E(\mathbf{6}^{2+*}/\mathbf{6}^{3+})$ and $E(\mathbf{6}^{2+*}/\mathbf{6}^{+})$. The results from this work allow us to estimate the value of the latter. As revealed by electrochemical studies, cluster $\mathbf{6}^{2+}$ exhibits a quasi-reversible reduction at -1.78 V versus $FeCp_2^{0/+}$, which can most reasonably be attributed to the reduction of $\mathbf{6}^{2+}$ to $\mathbf{6}^{+}$ [Reaction (8)]

$$[Cu_4(dcpm)_4(WS_4)]^{2+} + e \rightleftharpoons [Cu_4(dcpm)_4(WS_4)]^{+} \quad (8)$$

From the $E(\mathbf{6}^{2+}/\mathbf{6}^{+})$ value of -1.78 V (equal to -1.24 V versus a normal hydrogen electrode (NHE)), and the 0–0 transition energy $E_{0\text{-}0}$ of 2.36 eV (estimated from the position where the emission and the absorption spectra of $\mathbf{6}^{2+}$ overlap, cf. Figure 4), we estimate the reduction potential $E(\mathbf{6}^{2+*}/\mathbf{6}^{+})$ to be 1.12 V versus NHE according to Equation (1):

$$E(\mathbf{6}^{2+*}/\mathbf{6}^{+}) = E(\mathbf{6}^{2+}/\mathbf{6}^{+}) + E_{0\text{-}0} \quad (1)$$

This indicates that cluster $\mathbf{6}^{2+}$ in the excited state is a much better electron acceptor than in the ground state, and accounts for the reductive quenching of its emission by a series of amine donors with $E(D^+/D^0) \leq 1.07$ V versus NHE shown in Table 4. Interestingly, a three-parameter nonlinear least-squares fitting of the $\ln k_q'$ versus $E(D^+/D^0)$ plot[28] gives $E(\mathbf{6}^{2+*}/\mathbf{6}^{+})$ of 1.13 V versus NHE, in excellent agreement with the value of 1.12 V versus NHE obtained for $E(\mathbf{6}^{2+*}/\mathbf{6}^{+})$ from Equation (1).

Conclusion

We have shown here that metal–sulfur clusters derived from tetrathiometalates can exhibit intense photoluminescence with long emission lifetimes both in the solid state and in solution; this should stimulate further interest in the photophysical and photochemical properties of this fascinating family of heterometallic sulfido clusters. The present work also highlights that, besides their ligand properties, tetrathiometalates constitute a new class of anion templates for macrocycle formation; exploration of this property of tetrathiometalates may lead to the formation of intriguing metallamacrocycles with unusual conformations or properties. Moreover, the reactions of $[Cu_2(R_2PCH_2PR_2)_2(MeCN)_n]^{2+}$ with WS_4^{2-} in solution that afford the "fly-wheel" cluster $[Cu_3(dppm)_3(WS_4)]^+$ ($\mathbf{1}^+$, emissive in the solid state only) for R = Ph and the saddle-shaped cluster $[Cu_4(dcpm)_4(WS_4)]^{2+}$ ($\mathbf{6}^{2+}$, emissive in both the solid state and solution) for R = Cy reveal a striking influence of the steric/electronic factor of the phosphine ligands on the composition, structure, and photophysical properties of the cluster products. Finally, the observation of MMCT transitions for the d^0-d^{10} heterobimetallic cluster $\mathbf{6}^{2+}$ and its molybdenum analogue $\mathbf{5}^{2+}$, combined with their photoluminescence in solution, makes the two clusters unique candidates for investigating the reactivity of the MMCT excited state of a d^0-d^{10} heteronuclear metal complex.

Experimental Section

Gerneral: $(NH_4)_2MS_4$ (M = W and Mo, Aldrich) and the solvents for synthetic studies (AR grade) were used as received. The solvents for photophysical measurements were purified as described elsewhere.[29] $[Cu_2(dcpm)_2(MeCN)_2](ClO_4)_2$ was prepared by the literature method.[26] $Ag(PCy_3)ClO_4$ and $Au(PCy_3)Cl$ were prepared from the reactions of PCy_3 with $AgClO_4$ and $K[AuCl_4]$ (all purchased from Aldrich), respectively, by a similar preparation to that of $Ag(PCy_3)Cl$[30] and $Au(PPh_3)Cl$, respectively.[31] ^1H and ^{31}P NMR spectra were recorded on Bruker DPX300 and DRX500 FT-NMR spectrometers. Chemical shifts (δ) are reported relative to tetramethylsilane (^1H NMR) and 85% H_3PO_4 (^{31}P NMR). Infrared spectra were recorded on a Bio-Rad FTS-165 spectrometer, UV/Visible spectra on a Hewlett–Packard 8453 diode array spectrometer, and positive-ion FAB mass spectra on a Finnigan MAT95 mass spectrometer. Cyclic voltammograms were measured in acetonitrile containing 0.1M $(n\text{Bu}_4\text{N})PF_6$ with ferrocene as the internal standard [reference electrode: $Ag/AgNO_3$ (0.1M in acetonitrile), working electrode: glass carbon (Atomergic Chemetal V25), counter electrode: platinum gauze].

Preparation of $[Au_2(PCy_3)_2(MS_4)]$ (M = Mo: 2, W: 4): A mixture of $Au(PCy_3)Cl$ (0.23 g, 0.44 mmol) and $(NH_4)_2MS_4$ (0.22 mmol) in dichloromethane (20 mL) was stirred for 2 h to give a yellow suspension. The

0947-6539/01/0718-4004 $ 17.50+.50/0 *Chem. Eur. J.* **2001**, *7*, No. 18

suspension was filtered, and the filtrate was treated with excess diethyl ether, leading to precipitation of **2** or **4** as a yellow solid.

$[Au_2(PCy_3)_2(MoS_4)]$ (2): Yield: 60 %; ^{1}H NMR (300 MHz, $CDCl_3$): δ = 1.25 – 2.25 (m); $^{31}P\{^1H\}$ NMR (500 MHz, $CDCl_3$): $\delta = 66.98$ (s); IR (KBr): $\tilde{\nu} = 451\ cm^{-1}$ (MoS); FAB MS: m/z: 1179 $[M]^+$; elemental analysis calcd (%) for $C_{36}H_{66}P_2S_4MoAu_2 \cdot CH_2Cl_2$ (1263.93): C 35.12, H 5.42; found: C 35.24, H 5.55.

$[Au_2(PCy_3)_2(WS_4)]$ (4): Yield: 78 %; ^{1}H NMR (300 MHz, $CDCl_3$): δ = 1.24 – 2.25 (m); $^{31}P\{^1H\}$ NMR (500 MHz, $CDCl_3$): $\delta = 66.88$ (s); IR (KBr): $\nu = 439\ cm^{-1}$ (WS); FAB MS: m/z: 1184 $[M - Cy]^+$; elemental analysis calcd (%) for $C_{36}H_{66}P_2S_4WAu_2$ (1266.89): C 34.12, H 5.25; found: C 33.86, H 5.22.

Preparation of $[Ag_2(PCy_3)_2(WS_4)]$ (3): $(NH_4)_2WS_4$ (0.11 g, 0.3 mmol) was added to a solution of $Ag(PCy_3)ClO_4$ (0.29 g, 0.6 mmol) in dichloromethane (10 mL). The mixture was stirred for 6 h and then filtered. Addition of diethyl ether to the filtrate resulted in precipitation of **3** as a yellow solid in 43 % yield. ^{1}H NMR (300 MHz, $CDCl_3$): $\delta = 1.20 – 2.00$ (m); $^{31}P\{^1H\}$ NMR (500 MHz, $CDCl_3$): $\delta = 49.7$ (d, $J = 576$ Hz); IR (KBr): $\tilde{\nu}$ = 446 cm^{-1} (WS); FAB MS: m/z: 1089 $[M]^+$, 1006 $[M - Cy]^+$; elemental analysis calcd (%) for $C_{36}H_{66}P_2S_4WAg_2$ (1088.69): C 39.77, H 6.12; found: C 39.43, H 6.20.

Preparation of $[Cu_4(dcpm)_4(MS_4)](ClO_4)_2$ (M = Mo: $5 \cdot (ClO_4)_2$, W: $6 \cdot (ClO_4)_2$): A mixture of $[Cu_2(dcpm)_2(MeCN)_2](ClO_4)_2$ (0.21 g, 0.17 mmol) and $(NH_4)_2MS_4$ (0.088 mmol) in acetonitrile (20 mL) was stirred for 24 h under nitrogen, leading to formation of a yellow solution. The solution was filtered to remove any insoluble material, and then evaporated to dryness. The brown solid obtained was extracted with CH_2Cl_2. Concentration of the extract to 5 mL followed by addition of diethyl ether caused $5 \cdot (ClO_4)_2$ or $6 \cdot (ClO_4)_2$ to precipitate as a yellow solid.

$[Cu_4(dcpm)_4(MoS_4)](ClO_4)_2$ ($5 \cdot (ClO_4)_2$): Yield: 88 %; ^{1}H NMR (300 MHz, $CDCl_3$): $\delta = 1.25 – 2.20$ (m); $^{31}P\{^1H\}$ NMR (500 MHz, $CDCl_3$): $\delta = 6.44$ (s); IR (KBr): $\tilde{\nu} = 469\ cm^{-1}$ (MoS); FAB MS: m/z: 2212 $[M - ClO_4]^+$; elemental analysis calcd (%) for $C_{100}H_{184}P_8S_4O_8Cl_2MoCu_4$ (2311.61): C 51.96, H 8.03; found: C 51.56, H 8.13.

$[Cu_4(dcpm)_4(WS_4)](ClO_4)_2$ ($6 \cdot (ClO_4)_2$): Yield: 85 %; ^{1}H NMR (300 MHz, $CDCl_3$): $\delta = 1.25 – 2.20$ (m); $^{31}P\{^1H\}$ NMR (500 MHz, $CDCl_3$): $\delta = 6.58$ (s); IR (KBr): $\tilde{\nu} = 459\ cm^{-1}$ (WS); FAB MS: m/z: 2300 $[M - ClO_4]^+$; elemental analysis calcd (%) for $C_{100}H_{184}P_8S_4O_8Cl_2WCu_4 \cdot 2CH_2Cl_2$ (2569.37): C 47.76, H 7.39; found: C 47.80, H 7.40.

Photophysical measurements: Steady-state emission and excitation spectra were measured on a SPEX 1681 Flurolog-2 Model F111AI spectrofluorometer equipped with a Hamamatsu R928 PMT detector. The spectra at 77 K in the solid state and in MeOH/EtOH (4:1, v/v) glassy solution were recorded by loading the samples in a quartz tube located inside a quartz-walled optical Dewar flask filled with liquid nitrogen. For the solution spectra at 298 K, the samples in solution were subjected to four freeze-pump-thaw cycles before the measurement. The emission quantum yields were determined by the method of Demas and Crosby[32] with quinine sulfate in 1.0 N sulfuric acid as the standard ($\Phi_r = 0.546$).

X-ray structure determinations of clusters 2, 3, $5 \cdot (ClO_4)_2$, and $6 \cdot (ClO_4)_2$: Single crystals of $2 \cdot CH_2Cl_2$, $3 \cdot CH_2Cl_2$, $5 \cdot (ClO_4)_2 \cdot 2MeCN \cdot 2Et_2O$, and $6 \cdot (ClO_4)_2 \cdot EtOH$ were grown by slow diffusion of diethyl ether into a solution of **2** or **3** in dichloromethane, $5 \cdot (ClO_4)_2$ in acetonitrile, and $6 \cdot (ClO_4)_2$ in ethanol. For crystals $2 \cdot CH_2Cl_2$ ($0.20 \times 0.15 \times 0.10$ mm) and $3 \cdot CH_2Cl_2$ ($0.25 \times 0.20 \times 0.10$ mm), the data were collected at 301 K on a MAR diffractometer with a 300 mm image plate detector. The structures were solved by Patterson methods, expanded by Fourier methods (*PATTY*[33]), and refined by full-matrix least-squares on F by using the software package *TeXsan*[34] on a Silicon Graphics Indy computer. For crystals $5 \cdot (ClO_4)_2 \cdot 2MeCN \cdot 2Et_2O$ ($0.18 \times 0.16 \times 0.12$ mm) and $6 \cdot (ClO_4)_2 \cdot EtOH$ ($0.20 \times 0.20 \times 0.14$ mm), the data were collected at 294 K on a Bruker SMART CCD diffractometer. The structures were determined by the direct method and refined by full-matrix least-squares on F^2 by employing SHELXL-97 program on a PC computer. For each of the four crystals, graphite monochromatized $Mo_{K\alpha}$ radiation ($\lambda = 0.71073$ Å) was used, and all the non-hydrogen atoms were refined anisotropically, except for the solvent molecules of $2 \cdot CH_2Cl_2$ and $3 \cdot CH_2Cl_2$ (the non-hydrogen atoms of CH_2Cl_2 in $2 \cdot CH_2Cl_2$ and the C atom of CH_2Cl_2 in $3 \cdot CH_2Cl_2$ were refined isotropically). All the hydrogen atoms were placed at calculated positions without refinement.

Crystallographic data (excluding structure factors) for the structures reported in this paper have been deposited with the Cambridge Crystallographic Data Centre as supplementary publication no. CCDC-159439 (**2**), CCDC-159440 (**3**), CCDC-159441 ($5 \cdot (ClO_4)_2$), and CCDC-159442 ($6 \cdot (ClO_4)_2$). Copies of the data can be obtained free of charge on application to CCDC, 12 Union Road, Cambridge CB2 1EZ, UK (fax: (+44) 1223-336-033; e-mail: deposit@ccdc.cam.ac.uk).

Acknowledgements

This work was supported by The University of Hong Kong and the Hong Kong Research Grants Council [HKU 7298/99P and HKU 974/94P]. J.S.H. is grateful to The University of Hong Kong for a postdoctoral fellowship. We thank Prof. Kwok-Yin Wong and Dr. Guo-Bao Xu for assistance in the electrochemical measurements.

[1] a) A. Müller, E. Diemann, R. Jostes, H. Bögge, *Angew. Chem.* **1981**, *93*, 957; *Angew. Chem. Int. Ed. Engl.* **1981**, *20*, 934; b) R. H. Holm, *Chem. Soc. Rev.* **1981**, *10*, 455; c) D. Coucouvanis, *Acc. Chem. Res.* **1981**, *14*, 201; d) A. Müller, E. Diemann in *Comprehensive Coordination Chemistry, Vol. 2* (Eds.: G. Wilkinson, R. D. Gillard, J. A. McCleverty), Pergamon, Oxford, **1987**, p. 559; e) R. H. Holm, *Adv. Inorg. Chem.* **1992**, *38*, 1; f) H.-W. Hou, X.-Q. Xin, S. Shi, *Coord. Chem. Rev.* **1996**, *153*, 25; g) R. H. Holm, *Pure Appl. Chem.* **1998**, *70*, 931.

[2] J.-S. Huang, S. Mukerjee, B. M. Segal, H. Akashi, J. Zhou, R. H. Holm, *J. Am. Chem. Soc.* **1997**, *119*, 8662.

[3] a) K. Tanaka, Y. Imasaka, M. Tanaka, M. Honjo, T. Tanaka, *J. Am. Chem. Soc.* **1982**, *104*, 4258; b) D. Coucouvanis, P. E. Mosier, K. D. Demadis, S. Patton, S. M. Malinak, C. G. Kim, M. A. Tyson, *J. Am. Chem. Soc.* **1993**, *115*, 12193; c) L. J. Laughlin, D. Coucouvanis, *J. Am. Chem. Soc.* **1995**, *117*, 3118.

[4] a) V. W.-W. Yam, K. K.-W. Lo, W. K.-M. Fung, C.-R. Wang, *Coord. Chem. Rev.* **1998**, *171*, 17, and references therein; b) V. W.-W. Yam, E. C.-C. Cheng, Z.-Y. Zhou, *Angew. Chem.* **2000**, *112*, 1749; *Angew. Chem. Int. Ed.* **2000**, *39*, 1683.

[5] a) T. G. Gray, C. M. Rudzinski, D. G. Nocera, R. H. Holm, *Inorg. Chem.* **1999**, *38*, 5932; b) T. Yoshimura, K. Umakoshi, Y. Sasaki, S. Ishizaka, H.-B. Kim, N. Kitamura, *Inorg. Chem.* **2000**, *39*, 1765.

[6] C.-K. Chan, C.-X. Guo, R.-J. Wang, T. C. W. Mak, C.-M. Che, *J. Chem. Soc. Dalton Trans.* **1995**, 753.

[7] R. Schäfer, W. Kaim, J. Fiedler, *Inorg. Chem.* **1993**, *32*, 3199.

[8] a) A. Vogler, A. H. Osman, H. Kunkely, *Coord. Chem. Rev.* **1985**, *64*, 159; b) A. Vogler, H. Kunkely, *Coord. Chem. Rev.* **2000**, *200*, 991.

[9] a) J. C. Huffman, R. S. Roth, A. R. Siedle, *J. Am. Chem. Soc.* **1976**, *98*, 4340; b) E. M. Kinsch, D. W. Stephan, *Inorg. Chim. Acta* **1985**, *96*, L87; c) J. M. Charnock, S. Bristow, J. R. Nicholson, C. D. Garner, W. Clegg, *J. Chem. Soc. Dalton Trans.* **1987**, 303; d) R. G. Pritchard, L. S. Moore, R. V. Parish, C. A. McAuliffe, B. Beagley, *Acta Crystallogr. Sect. C* **1988**, *44*, 2022; e) F. Canales, M. C. Gimeno, P. G. Jones, A. Laguna, *J. Chem. Soc. Dalton Trans.* **1997**, 439.

[10] a) J. K. Stalick, A. R. Siedle, A. D. Mighell, C. R. Hubbard, *J. Am. Chem. Soc.* **1979**, *101*, 2903; b) J.-P. Lang, X.-Q. Xin, *J. Solid State Chem.* **1994**, *108*, 118.

[11] J.-P. Lang, K. Tatsumi, *Inorg. Chem.* **1998**, *37*, 6308.

[12] For example, the cone angle of PCy_3 is 170°, which is substantially larger than those of the phosphines such as PPh_3 (145°) and PEt_3 (132°) used in previous works (for cone angle values of phosphines, see: C. A. Tolman, *Chem. Rev.* **1977**, *77*, 313).

[13] A. Müller, H. Bögge, U. Schimanski, *Inorg. Chim. Acta* **1980**, *45*, L249.

[14] a) J. R. Nicholson, A. C. Flood, C. D. Garner, W. Clegg, *J. Chem. Soc. Chem. Commun.* **1983**, 1179; b) J. M. Manoli, C. Potvin, F. Sécheresse, S. Marzak, *J. Chem. Soc. Chem. Commun.* **1986**, 1557; c) C. Potvin, J.-M. Manoli, F. Sécheresse, S. Marzak, *Inorg. Chem.* **1987**, *26*, 4370; d) J. M. Manoli, C. Potvin, F. Sécheresse, S. Marzak, *Inorg. Chim. Acta* **1988**, *150*, 257; e) F. Sécheresse, S. Bernés, F. Robert, Y. Jeannin, *J. Chem. Soc. Dalton Trans.* **1991**, 2875; f) J. Lang, W. Zhou, X. Xin, K. Yu, *J. Coord. Chem.* **1993**, *30*, 173; g) C. Zhang, Y. Song, Y. Xu, H. Fun, G. Fang, Y. Wang, X. Xin, *J. Chem. Soc. Dalton Trans.* **2000**, 2823.

[15] The oxidation waves of $\mathbf{5}^{2+}$ and $\mathbf{6}^{2+}$ are irreversible and appear at $\sim$1.0 V versus $FeCp_2^{0/+}$.
[16] M. Kony, A. M. Bond, A. G. Wedd, *Inorg. Chem.* **1990**, *29*, 4521.
[17] R. Schäfer, W. Kaim, M. Moscherosch, M. Krejčik, *J. Chem. Soc. Chem. Commun.* **1992**, 834.
[18] The transient absorption spectrum of a mixture of $\mathbf{6}\cdot(ClO_4)_2$ and MV^{2+} in acetonitrile after flashing shows two peaks at about 390 and 600 nm characteristic of the $MV^{\bullet+}$ species (see: E. M. Kosower, J. L. Cotter, *J. Am. Chem. Soc.* **1964**, *86*, 5524). For the quenching by TMPD, intense bands at about 560 and 610 nm appear in the transient absorption spectrum of the mixture after flashing, indicating the formation of $TMPD^{\bullet+}$ (see: A. C. Albrecht, W. T. Simpson, *J. Am. Chem. Soc.* **1955**, *77*, 4454).
[19] E. Diemann, A. Müller, *Coord. Chem. Rev.* **1973**, *10*, 79.
[20] In the literature, the formation of macrocycles on anion templates is far less common than on cation templates, see for example: M. F. Hawthorne, Z. Zheng, *Acc. Chem. Res.* **1997**, 30, 267.
[21] a) N. Bresciani, N. Marsich, G. Nardin, L. Randaccio, *Inorg. Chim. Acta* **1974**, *10*, L5; b) D. M. Ho, R. Bau, *Inorg. Chem.* **1983**, *22*, 4079; c) M. P. Gamasa, J. Gimeno, E. Lastra, A. Aguirre, S. Garcia-Granda, *J. Organomet. Chem.* **1989**, *378*, C11; d) J. Diéz, M. P. Gamasa, J. Gimeno, A. Aguirre, S. Garcia-Granda, *Organometallics* **1991**, *10*, 380.
[22] a) A. M. M. Lanfredi, A. Tiripicchio, A. Camus, N. Marsich, *J. Chem. Soc. Chem. Commun.* **1983**, 1126; b) V. W.-W. Yam, W.-K. Lee, T.-F. Lai, *J. Chem. Soc. Chem. Commun.* **1993**, 1571; c) V. W.-W. Yam, W. K.-M. Fung, K.-K. Cheung, *Angew. Chem.* **1996**, *108*, 1213; *Angew. Chem. Int. Ed. Engl.* **1996**, *35*, 1100.
[23] S. Záliš, H. Stoll, E. J. Baerends, W. Kaim, *Inorg. Chem.* **1999**, *38*, 6101.
[24] C.-M. Che, M.-C. Tse, M. C. W. Chan, K.-K. Cheung, D. L. Phillips, K.-H. Leung, *J. Am. Chem. Soc.* **2000**, *122*, 2464.
[25] M. M. Savas, W. R. Mason, *Inorg. Chem.* **1987**, *26*, 301.
[26] C.-M. Che, Z. Mao, V. M. Miskowski, M.-C. Tse, C.-K. Chan, K.-K. Cheung, D. L. Phillips, K.-H. Leung, *Angew. Chem.* **2000**, *112*, 4250; *Angew. Chem. Int. Ed.* **2000**, *39*, 4084.
[27] See for example: a) K. Oldenburg, A. Vogler, *J. Organomet. Chem.* **1997**, *544*, 101; b) B. W. Pfennig, J. L. Cohen, I. Sosnowski, N. M. Novotny, D. M. Ho, *Inorg. Chem.* **1999**, *38*, 606; c) Y. J. Chen, C.-H. Kao, S. J. Lin, C.-C. Tai, K. S. Kwan, *Inorg. Chem.* **2000**, *39*, 189.
[28] V. W.-W. Yam, T.-F. Lai, C.-M. Che, *J. Chem. Soc. Dalton Trans*, **1990**, 3747.
[29] S.-W. Lai, M. C.-W. Chan, T.-C. Cheung, S.-M. Peng, C.-M. Che, *Inorg. Chem.* **1999**, *38*, 4046.
[30] G. A. Bowmaker, Effendy, P. J. Harvey, P. C. Healy, B. W. Skelton, A. H. White, *J. Chem. Soc. Dalton Trans.* **1996**, 2459.
[31] M. I. Bruce, B. K. Nicholson, O. B. Shawkataly, *Inorg. Synth.* **1989**, *26*, 324.
[32] J. N. Demas, G. A. Crosby, *J. Phys. Chem.* **1971**, *75*, 991.
[33] PATTY: P. T. Beurskens, G. Admiraal, G. Beurskens, W. P. Bosman, S. Garcia-Granda, R. O. Gould, J. M. M. Smits, C. Smykalla, "The DIRDIF Program System, Technical Report of the Crystallography Laboratory", University of Nijmegen (The Netherlands), **1992**.
[34] TeXsan: Crystal Structure Analysis Package, Molecular Structure Corporation, The Woodlands, Texas (USA), **1985** and **1992**.

Received: March 9, 2001 [F3121]

  0947-6539/01/0718-4006 $ 17.50+.50/0